



ORIGINAL ARTICLE

Solid supported microwave induced synthesis of imidazole–pyrimidine hybrids: Antimicrobial evaluation and docking study as 14DM-CPY51 inhibitors



Naziyanaz B. Pathan, Anjali M. Rahatgaonkar *

Chemistry Department, Institute of Science, R.T. Road, Civil Lines, Nagpur 440001, India

Received 10 December 2010; accepted 14 February 2011

Available online 19 February 2011

KEYWORDS

Cytochrome P450 (14DM)
CPY51;
Diphenylimidazolylpyrimidine;
Single crystal XRD;
Antifungal activity

Abstract As part of our exploration for new antifungal agents, substituted 4,5-diphenyl imidazolyl pyrimidine hybrids were synthesized. A series of substituted ethyl 1,2,3,6-tetrahydro-4-methyl-2-oxo/thioxo-6-phenyl-1-(4,5-diphenyl-1-*H*-imidazol-2-yl) pyrimidine-5-carboxylates have been studied for their binding active sites of cytochrome P450 14 α -sterol demethylase CPY51 enzyme. For comparison, the binding behavior of known 14DM selective (Fluconazole) and non-selective (Clotrimazole, Miconazole, Griesofulvin) drugs has also been studied. Synthesized compounds were screened for their *in vitro* antibacterial activity against *Staphylococcus aureus*, *Salmonella typhi*, *Pseudomonas aurogenosa* and *Klebsiella pneumoniae* and also antifungal activity against the opportunistic pathogens *Candida albicans*.

© 2011 Production and hosting by Elsevier B.V. on behalf of King Saud University. This is an open access article under the CC BY-NC-ND license (<http://creativecommons.org/licenses/by-nc-nd/3.0/>).

1. Introduction

Candida albicans, the most prevalent opportunistic fungal pathogen in humans, has been part of a general increase in the number of infection i.e. Candidiasis (Staib, 1965, 1969) ranging from superficial mucosal infection to life-threatening

systemic diseases in immuno compromised patients (with AIDS, Cancer, or Organ transplant). Azole compounds possessing N–C–N grouping display anti-inflammatory (Krimmel, 1961; Chem. Abstr., 1961a,b), hypotensive, anti-convulsant (Chem. Abstr., 1961a,b), amebicidal activity (Butter et al., 1967). The search for better antibacterial and antifungal agents with increased specificity towards bacterial as well as fungal enzymes remains a primary target in medicinal chemistry research. Many azoles target lanosterol 14 α -sterol demethylase and block ergosterol synthesis by interfering with the demethylation of its precursor (Fig. 1). Their broad therapeutic window, wide spectrum of activity and low toxicity has stimulated interest and revealed additional antimycobacterial activity associated with antifungal activity (Fioraventi et al., 1997a,b; Bobbarala and Naidu, 2009; Zhang et al., 2010).

* Corresponding author.

E-mail address: anjali_rahatgaonkar@yahoo.com (A.M. Rahatgaonkar).

Peer review under responsibility of King Saud University.



Production and hosting by Elsevier

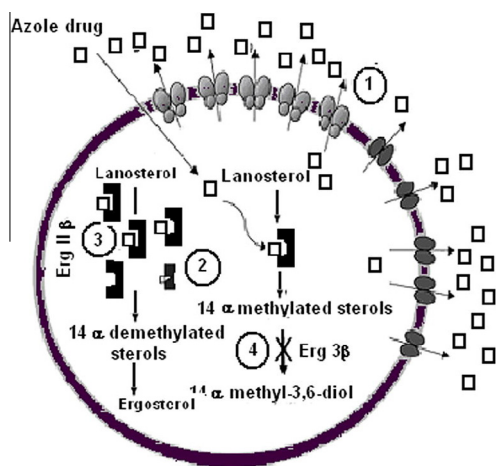


Figure 1 Mechanism of azoles drugs in biosynthesis pathway.

We thought it desirable to undertake the synthesis and bio-assay of compounds incorporating pyrimidine nucleus along with imidazole moiety in the same molecular framework to improve its specificity and efficacy against the microorganisms. Microwave (MW) irradiation (Singh et al., 2010) is currently used to carry out a wide range of reactions in short reaction time, with high productivity and stereo selectivity (Sharma and Mishra, 2010). We aimed to perform organic reactions under solvent free dry media conditions that avoid use of toxic solvents, thus preventing pollution (Melagraki et al., 2006). Microwave induced synthesis of the differently substituted ethyl 1,2,3,6-tetrahydro-4-methyl-2-oxo/thioxo-6-phenyl-1-(4,5-diphenyl-1-*H*-imidazol-2-yl) pyrimidine-5-carboxylate **3a–g** using acidic alumina has advantages over traditional methods. The dry media reaction proceeded rapidly in a forward direction and the time required for completion was highly reduced from hours to minutes.

The recent renewed interest in various imidazole analogues prompted the present study to demonstrate the use of synthesis and the utility of docking techniques has successfully verified for biological evaluation. Thus the application of newly synthesized derivatives saved time and human resource considerably. It is noteworthy to mention that this work provides a lead molecule, which can be further explored on the basis of present results to enhance the potential efficacy of pharmacophores.

2. Experimental

2.1. Chemistry

Differently substituted formylpyrimidines were made using analytical grade benzaldehyde, chlorobenzaldehyde, anisaldehyde, nitrobenzaldehyde (S.D. Fine Chem. 98%), Urea/thiourea, Absolute alcohol (99%), H₂SO₄ (Fischer 98%), DMF and POCl₃ (Thomas baker, 98%), Benzil (S.D. Fine Chem. 98%), Ammonium acetate and Glacial acetic acid (S.D. Fine Chem. 98%).

All solvents were distilled prior to use. TLC was performed on silica gel G. Melting points were determined by open capillary method and are uncorrected. IFB Domestic Microwave was used. ¹HNMR and ¹³CNMR spectra were recorded from

CDCl₃/DMSO-*d*₆ solution on a Bruker Avance II 400 (400 MHz) NMR Spectrometer. Chemical shifts are reported in ppm using TMS as an internal standard. IR spectra were obtained on a Shimadzu FTIR spectrophotometer using KBr discs. Mass spectra were recorded by using Shimadzu gas chromatograph coupled with QP5050 Spectrometer at 1–1.5 eV. X-ray diffraction analysis was carried out with FR590 MACH3 Single Crystal diffractometer. All the structures were resolved by direct methods using the solution program⁹ SHELX-97 in the WinGX package.

2.2. General procedure for synthesis of substituted ethyl 1,2,3,6-tetrahydro-4-methyl-2-oxo/thioxo-6-phenyl-1-(4,5-diphenyl-1-*H*-imidazol-2-yl) pyrimidine-5-carboxylates **3a–g**

2.2.1. Conventional method

Substituted ethyl 1-formyl-1,2,3,6-tetrahydro-4-methyl-6-phenyl-2-oxo/thioxopyrimidine-5-carboxylates **1a–g** (25 mmol), Benzil **2** (25 mmol, 5.25 g) and ammonium acetate (10 g) were dissolved in glacial acetic acid and refluxed for 10–12 h. After refluxing, the reaction mixture was left overnight and filtered to remove any precipitate. Water (300 mL) was then added to the filtrate and the first crop of crude material was obtained. The filtrate was neutralized with ammonium hydroxide and a second crop of the solid was collected. The two crops of the precipitate were combined, dried and recrystallized from ethanol.

2.2.2. Microwave irradiation method

Substituted ethyl 1-formyl-1,2,3,6-tetrahydro-4-methyl-6-phenyl-2-oxo/thioxopyrimidine-5-carboxylates **1a–g** (25 mmol), Benzil **2** (25 mmol, 5.25 g), ammonium acetate (10 g) and acidic alumina (1.0 g) were mixed thoroughly in an agate mortar. The mixture was placed in a beaker, 2-drops of glacial acetic acid was added. The beaker was kept in a microwave oven at maximum power level for 8 min with intermittent interval. The progress of reaction was monitored by TLC using benzene:ethyl acetate (8:2). The dried mass was diluted in cold water to dissolve acidic alumina and crude product was recovered, washed with ammonium hydroxide. The obtained mass was dried and recrystallized from ethanol (Scheme 1).

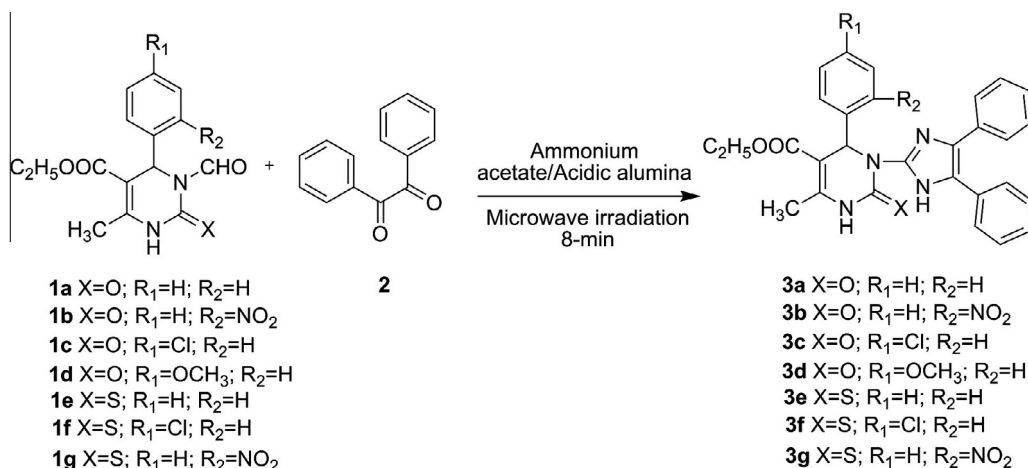
2.3. Computational evaluation: docking study

2.3.1. Methodology

All molecular techniques used in this manuscript were performed on Argus Lab ver. 4.0-work system. The starting 3D structure (Boscott and Grant, 1994) of the cytochrome P450sterol 14DM CPY51 of *C. albicans* was downloaded from the Protein Data Bank (<http://www.rcsb.org>) as PDB files (PDB entry: 1ea1).

2.3.2. 1ea1

The file containing the crystal structure of cytochrome P450 α -sterol demethylase (14DM) with its selective inhibitor i.e. Fluconazole (470TPF) in the active site (PDB entry 1ea1, six ligand) was downloaded. It is monomer structure with only chain A consisting of 449 residues. This chain A has 470YPF, water and 1 heme (HEM) groups. The chain A with residues, water and the hetero groups (HEM) within a radius of 5 Å was



Scheme 1

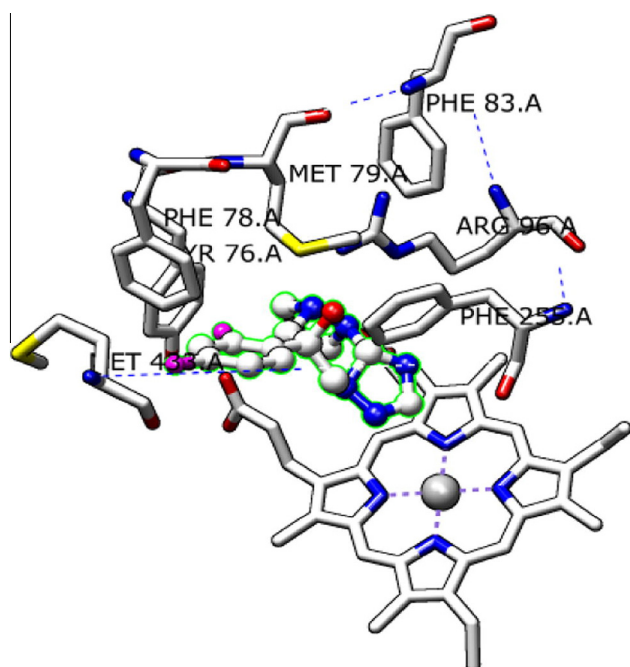


Figure 2 Active site residues of cytochrome P450 (14DM) CPY51 with Fluconazole (470TPF) hydrogens are suppressed for clarity.

refined and cleaned by checking the hybridization, valence of the ligand and introducing H-atoms to the protein residues. 1ea1 carries net charge 2 and 3590 atoms. The active sites of residues of 1ea1 are shown in (Fig. 2).

2.3.3. Docking and binding evaluation

In the automated module of Argus Lab ver. 4.0 work systems, the ligand was docked into the active site of cytochrome P450 14 α -sterol demethylase (14DM) from *C. albicans* using Argus dock with a fast, simplified potential of mean force (PMF). The docking is carried with flexible ligand into a rigid protein active site. The general procedure for docking process starts with the addition of energy minimized target ligand on the

enzyme. The active site and the ligand were specified in the program. The different starting parameters were optimized by using 15 \times 15 \times 15 box located at the centre of the target active site using a united atom (explicit hydrogen are not considered) potential of mean force (PMF) with a docking algorithm that has a population of 50 chromosomes and runs for 6000 generations. The process of docking is repeated until a constant value of docking score is reached. This takes about 12,000–18,000 generation. The final results are parameterized in terms of docking score in kcal/mol. The docked ligand–P450 (14DM) CPY51 complex is interpreted by looking at the H-bonding or hydrophobic interaction of the ligand with the amino acid residues in the active site. The same procedure was followed for docking of different substituted 4,5-imidazolyl pyrimidine into the active site of cytochrome P450 14 α -sterol demethylase CPY51 enzymes.

2.3.4. Validation of PMF method

To ensure the validation of the programme, before docking the test compounds, the docking of Fluconazole (470TPF) into the active site of P450 14DM was performed. This selective inhibitor of cytochrome P450 binds in the active site with a binding score of -9.1128 cal/mol. The docked structure of Fluconazole in the active site of cytochrome P450 is shown in (Fig. 2).

2.3.5. Docking of known selective and non-selective cytochrome P450 demethylase inhibitors into the active site of 1ea1

The non-selective behavior of Clotrimazole, Miconazole, Griesofulvin and selective behavior of Fluconazole towards cytochrome P450 (14DM) CY51 is in reasonable agreement with their binding energy (docking score) with 1ea1 as calculated from the docking of these compounds in 1ea1 active site. During binding of this known antifungal drug in the binding pocket of cytochrome P450, the conformational placement of amino acid residues in the active site is observed.

2.3.6. Docking of imidazolylpyrimidine derivatives into active site of 1ea1

The docking of synthesized substituted 4,5-diphenyl imidazolyl pyrimidine derivatives (Scheme 1) 3a–g in 14DM active site has been studied.

2.4. Biology

2.4.1. *In vitro* antibacterial activity

As the sensitivity was not observed at conc. $< 100 \mu\text{g disc}^{-1}$, the antibacterial activity of compounds **3a–g** has been assayed at concentration of $100 \mu\text{g disc}^{-1}$ against strains of Gram +ve and Gram –ve pathogenic bacteria (*Salmonella typhi*, *Pseudomonas aurogenosa*, *Klebsiella pneumoniae* and *Staphylococcus aureus*). Initially, susceptibility testing was carried out by measuring the inhibitory zone diameter on Muller–Hinton agar, with conventional paper disc diffusion method (Fioraventi et al., 1997a,b), and the inhibitory zone diameters were read and rounded off to the nearest whole numbers (mm) for analysis. The inhibitory effects of compounds **3a–g** against these organisms were compared with standard drug i.e. Norfloxacin.

2.4.2. *In vitro* antifungal activity

As the sensitivity was not observed at conc. $< 100 \mu\text{g disc}^{-1}$, the antifungal activities of compounds **3a–g** have been assayed *in vitro* at a concentration $100 \mu\text{g disc}^{-1}$ against *C. albicans*. Griesofulvin was used as standard fungicide for the antifungal

test. Muller–Hinton agar was used as basal medium for test fungi (Fioraventi et al., 1997a,b). Glass Petri dishes were sterilized and 10 ml of sterilized melted MH agar medium (45°C) was poured into each Petri dish. After solidification of the medium, small portion of mycelium of *C. albicans* was spread carefully over the centre of each MH agar plate with the help of spreader. Thus, fungus was transferred to each plate. The plates were then incubated at (27°C) and after half an hour of incubation they were ready for use. The prepared discs of test sample were placed gently with sterile forceps on the solidified agar plate, freshly seeded with the test organisms. The plates were then incubated at 37.5°C for 24 h. Dimethyl formamide (DMF) was used as a solvent to prepare desired solutions of the compounds initially.

3. Results and discussion

3.1. Chemistry

Substituted ethyl 1,2,3,6-tetrahydro-4-methyl-2-oxo/thioxo-6-phenyl-1-(4,5-diphenyl-1-*H*-imidazol-2-yl) pyrimidine-5-car-

Table 1 Characteristic spectral data of synthesized compounds **3a–g**.

Entry	m.p. ($^\circ\text{C}$)	IR (cm^{-1})	Chemical shifts (δ_{H}) in ppm	Chemical shifts (δ_{C}) in ppm	Yield (%)		Molecular formula	Mass [M^+]
					MW	Conv.		
3a	160	3198 (N–H), 1499 (C=C), 1435 (C=N)	1.1 (t, 3H, CH_3 , $J = 8$), 2.3 (s, 3H, CH_3), 4.2 (q, 2H, CH_2 , $J = 4.8$), 5.1 (s, 1H, Ar–H), 8.9 (s, 1H, N–H)	13.7, 17.7, 54.4, 59.0, 99.7, 127.2, 128.6, 129.5, 129.3, 132.7, 134.2, 147.1, 148.2, 158.8, 165.3, 167.1, 194.1	79	64	$\text{C}_2\text{H}_{26}\text{N}_4\text{O}_3$	478
3b	210	3190 (N–H), 1493 (C=C), 1430 (C=N)	1.3 (t, 3H, CH_3 , $J = 8$), 2.1 (s, 3H, CH_3), 4.1 (q, 2H, CH_2 , $J = 4.8$), 5.4 (s, 1H, Ar–H), 8.7 (s, 1H, N–H)	13.5, 17.9, 54.2, 59.0, 99.6, 127.1, 128.6, 129.5, 129.3, 132.3, 134.0, 147.8, 148.5, 158.8, 165.7, 167.1, 194.3	78	64	$\text{C}_{29}\text{H}_{25}\text{N}_4\text{O}_3\text{Cl}$	523
3c	180	3198 (N–H), 1549 (C=C), 1435 (C=N)	1.4 (t, 3H, CH_3 , $J = 7.6$), 2.4 (s, 3H, CH_3), 4.0 (q, 2H, CH_2 , $J = 4.2$), 5.2 (s, 1H, Ar–H), 9.2 (s, 1H, N–H)	13.4, 17.6, 54.3, 59.2, 99.7, 127.2, 128.4, 129.5, 129.6, 132.7, 134.6, 147.1, 148.2, 158.53, 167.1, 194.8	69	62	$\text{C}_{29}\text{H}_{25}\text{N}_5\text{O}_5$	512
3d	240	3195 (N–H), 1489 (C=C), 1469 (C=N)	1.1 (t, 3H, CH_3 , $J = 8.2$), 2.3 (s, 3H, CH_3), 3.7 (s, 3H, OCH_3), 4.0 (q, 2H, CH_2 , $J = 4.8$), 5.3 (s, 1H, Ar–H), 8.9 (s, 1H, N–H)	13.2, 17.6, 54.1, 59.3, 99.7, 127.2, 128.6, 129.5, 129.3, 132.7, 134.1, 147.1, 148.2, 158.8, 165.3, 167.1, 194.5	72	65	$\text{C}_{30}\text{H}_{28}\text{N}_4\text{O}_4$	508
3e	190	3198 (N–H), 1494 (C=C), 1430 (C=N)	1.3 (t, 3H, CH_3 , $J = 8$), 2.2 (s, 3H, CH_3), 4.2 (q, 2H, CH_2 , $J = 4.8$), 5.5 (s, 1H, Ar–H), 9.5 (s, 1H, N–H)	13.3, 17.7, 54.4, 59.0, 99.2, 127.4, 128.6, 129.5, 129.3, 132.7, 134.2, 147.1, 148.2, 158.8, 165.3, 167.1, 194.3	78	65	$\text{C}_{29}\text{H}_{26}\text{N}_4\text{O}_2\text{S}$	494
3f	195	3200 (N–H), 1493 (C=C), 1433 (C=N)	1.2 (t, 3H, CH_3 , $J = 8$), 2.4 (s, 3H, CH_3), 4.1 (q, 2H, CH_2 , $J = 4.8$), 5.3 (s, 1H, Ar–H), 9.3 (s, 1H, N–H)	13.7, 17.7, 54.4, 59.3, 99.7, 127.2, 128.6, 129.5, 129.3, 132.7, 134.0, 147.1, 148.2, 158.8, 165.3, 167.1, 194.4	75	63	$\text{C}_{29}\text{H}_{25}\text{N}_4\text{O}_2\text{SCl}$	528
3g	220	3205 (N–H), 1495 (C=C), 1435 (C=N)	1.3 (t, 3H, CH_3 , $J = 8$), 2.3 (s, 3H, CH_3), 4.0 (q, 2H, CH_2 , $J = 4.6$), 5.1 (s, 1H, Ar–H), 9.6 (s, 1H, N–H)	13.4, 17.6, 54.4, 59.0, 99.3, 127.2, 128.6, 129.5, 129.3, 132.7, 134.0, 147.1, 148.2, 158.8, 165.3, 167.1, 194.7	67	60	$\text{C}_{29}\text{H}_{25}\text{N}_5\text{O}_4\text{S}$	539

boxylates **3a–g** were synthesized by conventional and non-conventional methods. Condensation of substituted ethyl 1-formyl-1,2,3,6-tetrahydro-4-methyl-6-phenyl-2-oxo/thioxo-pyrimidine-5-carboxylate **1a–g** and Benzil **2** using acidic alumina and ammonium acetate under solvent free microwave irradiation was adopted preferentially as it was an environmentally friendly and economically profitable method that reduced the time of reaction from hours to minutes (Table 1).

Table 2 Crystal and experimental data for the title compound.

Chemical formula	C ₂₉ H ₂₆ N ₄ O ₃
Molecular weight (g/mol)	478
Crystal size	0.2 × 0.24 × 0.05
Crystal system	Triclinic
Space group	\bar{P}
Unit cell dimensions	
<i>a</i>	4.1532
<i>b</i>	4.518
<i>c</i>	5.25
α	76
β	88
γ	104
Volume	98.507
(Cal.) Density (g/cm ⁻³)	0.206
<i>F</i>	(000) 252
Index range (<i>h</i> , <i>k</i> , <i>l</i>)	h (0–5), k (0–5), l (0–4)
Absorption correction	Integration
Absorption coefficient	0.053
Goodness of fit on <i>F</i> ²	0.98
Final <i>R</i> indices [<i>I</i> > 2σ (<i>I</i>)]	0.03
Temperature	299 K
Radiation	Mo Kα
λ	0.70930
<i>R</i>	0.0394
<i>R</i> _w	0.0828

The structure of ethyl 1,2,3,6-tetrahydro-4-methyl-2-oxo-6-phenyl-1-(4,5-diphenyl-1-*H*-imidazol-2-yl) pyrimidine-5-carboxylate **3a** was supported by elemental analysis, IR, ¹HNMR, ¹³CNMR, MASS spectral data. IR spectra exhibited an N–H absorption band at 3198 cm⁻¹, ester carbonyl group at 1750 cm⁻¹, C=C stretch at 1495 cm⁻¹, C=N stretch at 1435 cm⁻¹. ¹HNMR (CDCl₃/DMSO_d₆) was nicely resolved and showed the appearance of N–H proton as a characteristic singlet at δ 8.9 and the aromatic protons as a multiplet at δ 7.1–7.9 (Table 1). The appearance of multiplets of 14 protons at δ 7.2–8.5 showed the presence of two more phenyl rings attached to the basic moiety; the disappearance of the –CHO peak from δ 10.2–10.4 confirmed the formation of product **3a**. ¹³CNMR showed the disappearance of peak of H–C=O in compound **3a**; the appearance of peak of N–C–N at δ 134.0 confirmed its structure.

The construction of the imidazole ring on *N*-formylpyrimidine **3a–g** was performed in a facile manner affording the final compounds in overall good yield with high purity. A simple

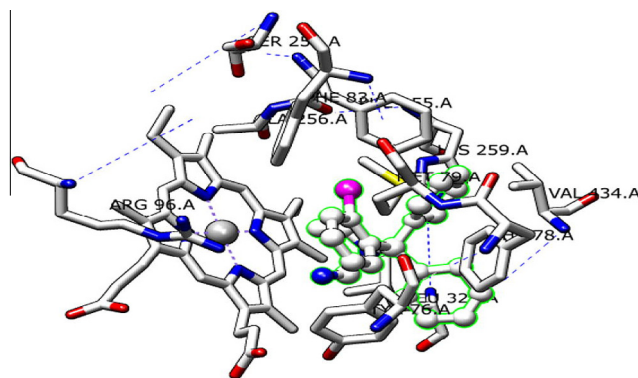


Figure 4 Active site residues of cytochrome P450 (14DM) CPY51 with clotrimazole hydrogens are suppressed for clarity.

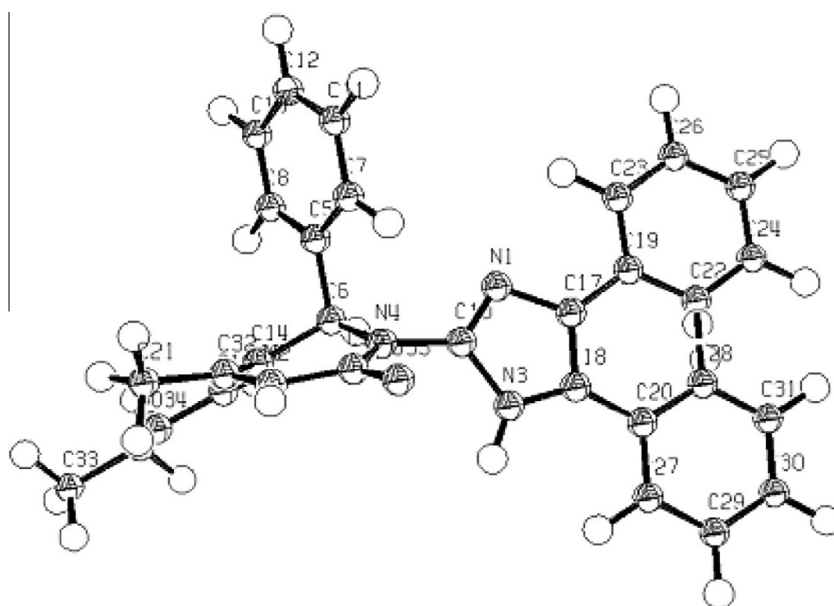


Figure 3 An ORTEP drawing of the molecule **3a** showing the atomic numbering system.

strategy was developed for the synthesis of 4,5-diphenyl imidazolylpyrimidine derivatives **3a–g** in which the two aryl rings are placed at C-4 and C-5 carbon on the opposite faces of the nearly planar imidazole ring. The structural arrangement and characterization of compound **3a** was proved by X-ray crystal analysis.

3.1.1. A-single crystal XRD **3a**

Yellow coloured needle shape single crystals suitable for X-ray diffraction were grown from methanol using the slow evaporation technique. Diffraction intensity data were collected with a FR590 MACH3 single crystal diffractometer using Mo $K\alpha$ monochromated radiation ($\lambda = 0.70930$) at room temperature (299 K). Crystal data, data collection and structure refinement for the compound are listed in (Table 2). The final atomic coordinates for all atoms and a complete listing of bond distance and angles are tabulated.

An integration type of absorption correction was applied to data sets. The structure was resolved by direct methods using the solution program SHELXS97 in the WinGX package

(Sheldrick, 1997) and refined by a full-matrix least-squares procedure on F^2 using SHELXS97. All non-hydrogen atoms were refined, first with isotropic and then anisotropic parameters. Hydrogen atoms bonded to carbon were included using a riding model, starting from calculated positions. An ORTEP-3 (Farrugia, 1997) drawing of the molecule with the atomic numbering scheme is shown in (Fig. 3).

3.2. Docking study

Clotrimazole binds in the active site of cytochrome P450 (1ea1) mainly through hydrophobic interaction. Clotrimazole mainly has two phenyl ring attached to the same carbon atom. Phenyl ring (C) is surrounded by VAL 434, HIS 59, PHE 255, and ALA 256; phenyl ring (D) is enveloped by TYR 76 and LEU 321 (Fig. 4). It also contains one *p*-chloro substituted phenyl ring which approaches PHE 78, MET 79, PHE 83, and ARG 96. Therefore –Cl substituted phenyl ring present on Clotrimazole through π – π interaction with amino acid residues kept in place in active site of cytochrome P450, increases the binding energy, by -15.4404 kcal/mol (Table 3).

These compounds contain a central core imidazole ring having N–C–N bonding, characteristic ofazole antifungal drugs. Two aryl rings at C-4 and C-5 carbon on the opposite faces of two nearly planar imidazole ring result in decrease in steric repulsion on the opposite faces of the imidazole ring providing for free rotation of the two aryl rings. All the synthesized imidazolyl pyrimidine molecules show binding in the active site of P450 (14DM) CPY51 with binding score between -7.86 and -12.45 kcal/mol (Table 3). Compounds **3a**, **3b**, **3c**, **3d**, **3f** show the highest binding with P450 (14DM) in comparison to selective drug i.e. Fluconazole. Further rationalization of modes of P450 (14DM) CPY51 has been based upon the amino acid residues present around the ligand, in the active site pocket of 1ea1. On the basis of structural features essential for binding in the cavity, the imidazolyl pyrimidine molecules could be divided into three segments: C-4 phenyl, C-5 phenyl, C-2 substituted pyrimidine. The residues surrounding each phenyl group and C-2 substituted pyrimidine molecules have been determined (Table 4).

Table 3 Binding score of known selective and non-selective drugs and 4,5-diphenyl imidazolylpyrimidine derivatives (DPIP) with P450 (14DM) CPY51.

Entry	Ligand	Binding score (Kcal/mol)
1	Clotrimazole _(non-selective)	-15.4404
2	Miconazole _(non-selective)	-12.9387
3	Griesofulvin _(non-selective)	-9.2418
4	Fluconazole _(selective)	-9.1128
5	3a	-11.98
6	3b	-12.4528
7	3c	-12.2386
8	3d	-11.98
9	3e	-9.9351
10	3f	-12.0495
11	3g	-7.8615

Table 4 Amino acid residues around each segment of imidazolylpyrimidine derivatives docked into cytochrome P450 (14DM) CPY51.

Entry	Ligand	Amino acid residues surrounding		
		C-2 substituted pyrimidine ring	C-4 phenyl ring	C-5 phenyl ring
1	3a	ALA 397, ILE 401, LEU 315, LYS 312, GLU 308	PHE 387, ARG 393, ALA 389, GLY 388	ARG 381, ASN 380, LEU 378, ASP 377, TRP 384
2	3b	GLY 388, ILE 385, ARG 393, TRP 384, AR 381, ASN 380, PRO 386	LEU 315, LYS 312, LEU 311, PHE 387	ILE 401, GLU 308, LEU 378, ASP 377
3	3c	MET 253, LEU 152, GLU 98, GLU 94	PHE 89	LEU 229, VAL 228, MET 225, MET 249
4	3d	GLU 308, ALA 397, ALA 398, ILE 401	ASP 377, LEU 378, LYS 312	TRP 384, LEU 315, PHE 387, ARG 393
5	3e	ALA 350, ILE 27, ILE 351, ASP 25, GLY 28, GLN 31, ARG 354	ASN 428, HIS 430, ILE 322	HIS 318, TRP 267, LEU 317, HIS 363
6	3f	GLU 308, LEU 311, LYS 312, ILE 401, LEU 315, ALA 397, ALA 398	PRO 386, ARG 393, ILE 385, PHE 387, GLY 388	TRP 384, LEU 378, ASP 377, ARG 381, ASN 380
7	3g	LYS 233, VAL 232, ALA 23, PHE 241, VAL 88, PHE 89	ARG 223	LEU 229, VAL 228

The most prominent binding is observed in ligands **3b**, **3c** and **3f** as compared to their other substituent. For ligands **3b** and **3f**, the two phenyl rings are stabilized by hydrophobic interaction. In case of **3b**, C-4 phenyl ring is surrounded by LEU 315, LEU 311, LYS 312 and PHE 387. C-5 phenyl ring is surrounded by LEU 378, ILE 401, GLU 308, ASP 377 and C-2 substituted pyrimidine is enveloped by GLY 388, ILE 385, ARG 393, TRP 384, ARG 381, ASN 380, PRO

386 (Fig. 5). In **3f**, C-4 phenyl ring is surrounded by PRO 386, ARG 393, ILE 385, PHE 387 and GLY 388. The C-5 phenyl ring is surrounded by TRP 384, LEU 378, ASP 381, ASN 380; the C-2 substituted pyrimidine molecule is surrounded by GLU 308, LEU 311, LYS 312, ILE 401, LEU 315, ALA 397, ALA 398 (Fig. 6). These C-2 substituted pyrimidine have halogen -Cl atom as a substituent of phenyl ring: in compound **3b** and **3f** the binding score is increased by -12.4528 and

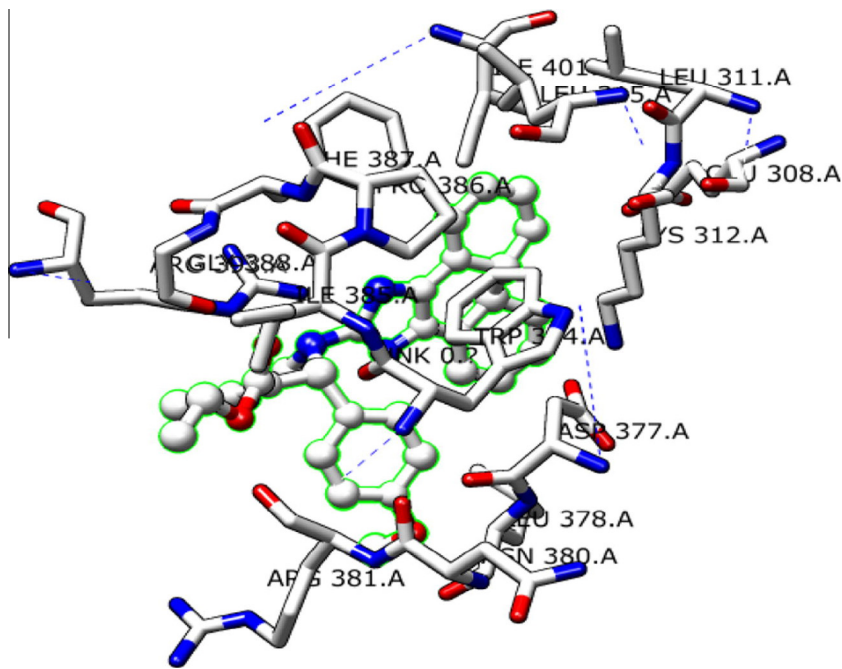


Figure 5 Docked in the active site of cytochrome P450 **3b**.

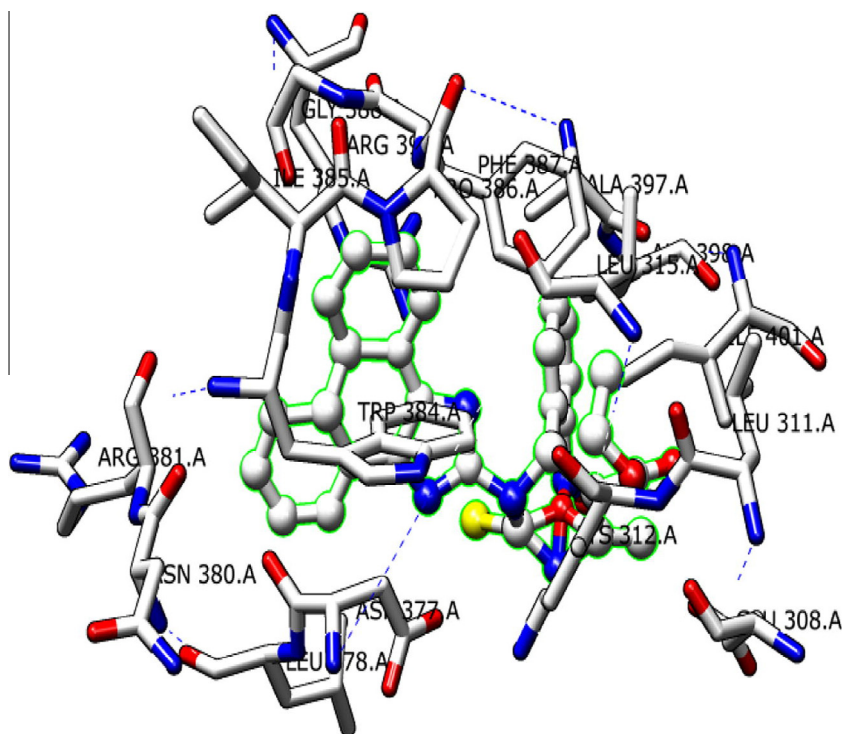


Figure 6 Docked in the active site of cytochrome P450 **3f**.

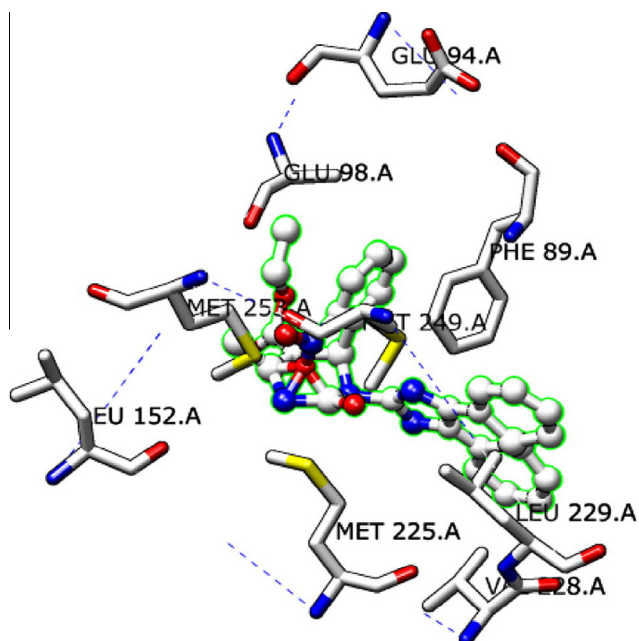


Figure 7 Docked in the active site of cytochrome P450 **3c**.

–12.0495 kcal/mol respectively through π – π interaction with amino acid residues kept in active site of cytochrome P450. For ligand **3c**, C-4 phenyl ring approaches PHE 89. C-5 phenyl ring is surrounded by LEU 229, VAL 228, MET 225, MET 249, GLU 98. The C-2 substituted pyrimidine having NO₂ as substituent of phenyl ring are surrounded by MET 253, LEU 152, GLU 94: the docking score is –12.2386 kcal/mol (Fig. 7).

3.3. Biology

3.3.1. *In vitro* antibacterial and antifungal activities

The screening results revealed that in addition to **3a–c**, the compound **3d** was found to be the most active against *S. aureus* amongst all the tested compounds. *S. typhi* is highly sensitive to the compound **3b** and **3e–g** while moderately sensitive to Compounds **3a** and **3c**. The results depicted in Table 5 suggested that *P. aurogenosa* and *K. pneumoniae* are highly resistant to the synthesized compounds. *In vitro* antifungal studies revealed that the compounds **3b** and **3c** displayed significant activity while rest of the compounds showed moderate to low activity (Table 5).

Similarly preliminary studies in order to verify how the synthesized azole compounds interact at the target enzyme cytochrome P450-dependent lanosterol 14 α -demethylase (P450 14DM, CPY51) in the ergosterol biosynthesis pathway have been carried out by computational approach and structure–activity relationship.

3.3.2. Structure–activity relationship

A comparative study involving the interaction of known antimicrobial drug viz. Clotrimazole, Miconazole, Fluconazole, and Griesofulvin in the active site pocket of cytochrome P450 (1ea1) was made for better understanding of their antibacterial and antifungal action. Structure–activity relationship, a powerful stencil used for tailoring effective lead molecules, was studied. We tested the entire synthesized compounds against bacteria and fungus with moderate to high antimicrobial activity. All compounds can be generalized into a single frame work and expected to show their potency as synthetic inhibitor, depending upon the structural features essential for binding in the cavity of cytochrome P450 (1ea1). All newly synthesized molecules (**3a–g**) could be divided into three segments viz. imidazole central core structure (ring A), characteristics substituted pyrimidine nucleus (ring B) and two phenyl rings (rings C and D). Our hybrid molecule considered as a template scaffold in which one can insert substituted aromatic ring as a substituent of ring B to enhance the specificity towards microorganism as antifungal activities. These hybrid molecules possesses ring A as imidazole subunit, ring B constitute substituted pyrimidine ring at C-2 position of imidazole ring while the attached two phenyl ring at C-4 and C-5 position of main imidazole moiety raised antifungal activity (Fig. 8).

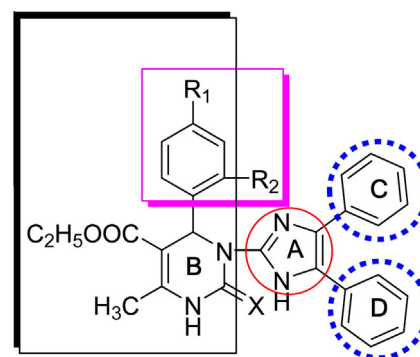


Figure 8 Structure–activity relationship.

Table 5 Antimicrobial-screening results of synthesized compounds **3a–g**.

Entry	<i>S. aureus</i> (mm)	<i>S. typhi</i> (mm)	<i>P. aurogenosa</i> (mm)	<i>K. Pneumoniae</i> (mm)	<i>C. albicans</i> (mm)
3a	10	9.0	9.0	12.0	9.0
3b	10	12	–	12.0	12.0
3c	9.0	9.0	12.0	10.0	13.0
3d	12.0	–	10.0	15.0	–
3e	6.0	13.0	12.0	9.0	–
3f	6.0	11.0	6.0	18.0	12.0
3g	7.0	13.0	10.0	8.0	9.0
N	10.0	11.0	22.0	24.0	–
G	–	–	–	–	11.0

N, Norfloxacin; G, Griesofulvin.

It is interesting to note that the compounds **3b**, **3c** and **3f** exhibit significant antifungal activity revealing that the presence of electron withdrawing groups like $-\text{Cl}$, NO_2 as substituent at different position on aromatic ring attached to ring B improved the efficacy of the compounds. The two phenyl rings are essential for modulation of the hydrophobic interaction which enhanced its antifungal activity. Other compounds, exhibited moderate activity against fungi and bacteria due to the presence of $-\text{OCH}_3$ and $-\text{OH}$ group on substituted aromatic ring.

4. Conclusion

We report herein, facile synthesis of several biologically active imidazolylpyrimidine derivatives under solvent free condition and none conventionally, docking studies and experimental observation suggest that they could constitute the unique class of lead inhibitor. Diversity of substitution on the skeleton of pyrimidine scaffold leads to significantly modulated selectivity in the lead active site cavity. Substituted *p*-chloro phenyl ring at C-4 position of pyrimidine or attached to C-2 carbon of imidazole ring enhances the binding capacity and selectivity and results in enhanced discrimination with cytochrome P450demethylase CPY 51 active site. A joint molecule of imidazolylpyrimidine improves specificity and efficacy of both nuclei against microorganism. The dry media reaction proceeded rapidly in a forward direction and time required for completion was highly reduced from hours to minutes. The negative bonding score, relatively short and easy synthesis of these molecules make them attractive candidates for further exploration. Further computation evaluation was validated by experimental study through ecofriendly method without using toxic solvent.

Acknowledgements

Authors acknowledge Department of Pharmacy, Nagpur for IR spectra, SAIF, Chandigarh for ^1H NMR, ^{13}C NMR spectra, University of Pune for the Mass analysis and RSIC, Kolkata for measurement of X-ray diffraction data.

Appendix A. Supplementary data

Crystallographic data for the structural analysis reported in this paper have been deposited with the Cambridge Crystallographic Data Centre as CCDC 687592. Copies of the information may be obtained free of charge from Director, CCDC, 12, Union Road, CambridgeCBZ1EZ, UK. (Fax: +44 1223 336033; e-mail: deposit@ccdc.cam.ac.uk, homepage: <http://www.ccdc.cam.ac.uk>).

Supplementary data associated with this article can be found, in the online version, at doi:10.1016/j.arabjc. 2011.02.013.

References

- Bobbarala, V., Katikala, P.K., Naidu, K.C., Penumajji, S., 2009. Ind. J. Sc. Tech. 20, 87–90.
- Boscott, P.A., Grant, G.H., 1994. J. Mol. Graph. 12, 185.
- Butter, K., Howes, H.L., Lynch, J.E., Pioie, D.K., 1967. J. Med. Chem. 10, 891.
- Chem. Abstr., 1961a. 55, 15513d:Krimmel, C.P., Patent US, 2, 969, 369, 1961.
- Chem. Abstr., 1961b. 55, 23503h: Turkevich, N.M., Lyman (Med. Inst., Lvov), 1961. Zhur. Obstichei Khim. 31, 1635–1640.
- Fioraventi, R., Biava, M., Porretta, G.C., Artico, M., Lampis, G., Deidda, D., Pompei, R., 1997a. Med. Chem. Res. 7, 87.
- Fioraventi, R., Biava, M., Porretta, G.C., Sleiter, G., Ettore, A., Deidda, D., Pompei, R., 1997b. Med. Chem. Res. 7, 228.
- Farrugia, L.J., 1997. J. Appl. Cryst. 30, 565.
- Krimmel, C.P., Patent US, 2, 969, 369, 1961.
- Melagraki, G., Afantitis, A., Makridima, K., Sarimveis, H., Igglessi-Markopoulou, O., 2006. J. Mol. Model. 12, 297.
- Singh, V., Kumari, P.L., Tiwari, A., Pandey, S., 2010. J. Appl. Polym. Sci. 117, 3107–3728.
- Sharma, A.K., Mishra, A.K., 2010. Adv. Mat. Lett. 1 (1), 59–66.
- Sheldrick, G.M., 1997. SHELX-97 Programme for Solution and Refinement of Crystal Structure. University of Gottingen, Germany.
- Staib, F., 1969. Proteolysis and pathogenicity of *Candida albicans* strains. Mycopathol. Mycol. Appl. 37, 345–348 (medicine).
- Staib, F., 1965. Serum-protein as nitrogen source for yeast like fungi *sabouraudia* 4, 187–193 (medicine).
- Zhang, Y., Rao, A., Muend, S., 2010. Antimicrob. Agent Chemother. 54 (12), 5062–5069.